Title: Aberrant subcutaneous adipogenesis precedes adult metabolic dysfunction in an ovine model of polycystic ovary syndrome (PCOS)

Authors: Katarzyna J. Siemienowicz[a,b]*, Flavien Coukan[b], Stephen Franks[c], Mick T. Rae[b], W. Colin Duncan[a]

Affiliations: [a]MRC Centre for Reproductive Health, The University of Edinburgh, Edinburgh EH16 4TJ, UK; [b]School of Applied Sciences, Edinburgh Napier University, Edinburgh EH11 4BN, UK; [c]Institute of Reproductive and Developmental Biology, Imperial College, London, UK.

***Corresponding Author:**
Katarzyna J. Siemienowicz
School of Applied Sciences,
Edinburgh Napier University,
Edinburgh EH11 4BN, UK
Tel: +44 (0)131 455 3458
E-mail: k.siemienowicz@napier.ac.uk

Abstract

Polycystic ovary syndrome (PCOS) affects over 10% of women. Insulin resistance, elevated free fatty acids (FFAs) and increased adiposity are key factors contributing to metabolic dysfunction in PCOS. We hypothesised that aberrant adipogenesis during adolescence, and downstream metabolic perturbations, contributes to the metabolic phenotype of adult PCOS. We used prenatally androgenized (PA) sheep as a clinically realistic model of PCOS. During adolescence, but not during fetal or early life of PA sheep, adipogenesis was decreased in subcutaneous adipose tissue (SAT) accompanied by decreased leptin, adiponectin, and increased FFAs. In adulthood, PA sheep developed adipocyte hypertrophy in SAT paralleled by increased expression of inflammatory markers, elevated FFAs and increased expression of genes linked to fat accumulation in visceral adipose tissue. This study provides better understanding into the pathophysiology of PCOS from puberty to adulthood and identifies opportunity for early clinical intervention to normalise adipogenesis and ameliorate the metabolic phenotype.

Keywords: polycystic ovary syndrome, adipose tissue, adipogenesis, prenatal programming, metabolism, androgens

1. Introduction

Polycystic ovary syndrome (PCOS) is a common disorder, affecting up to 10% of women of reproductive age (Fauser et al., 2012). Women with PCOS have increased risks of hyperinsulinemia, insulin resistance, obesity, dyslipidemia and fatty liver (Fauser et al., 2012; Moran et al., 2015; Teede et al., 2010). Metabolic comorbidities associated with the syndrome worsen with age and pose a significant health and economic burden (Jason, 2011; Teede et al., 2010).

Overweight/obese women with PCOS have increased abdominal adiposity when compared with BMI-matched controls, correlated with an adverse metabolic profile (Puder et al., 2005; Yildirim et al., 2003). In addition, women with PCOS have adipose tissue dysfunction, independent of obesity (Carmina et al., 2005; Echiburú et al., 2018; Manneras-Holm et al., 2010; Seow et al., 2009; Wang et al., 2012). Although studies using animal models of PCOS have also indicated adipose tissue abnormalities, the data is inconclusive (Keller et al., 2014; Puttabyatappa et al., 2018; Veiga-Lopez et al., 2013). Insulin and androgens, both typically increased in PCOS, affect adipogenesis and adipose tissue function (Chazenbalk et al., 2013; Klemm et al., 2001), and thus are likely to play an important role in adipose tissue dysfunction in PCOS. White adipose tissue (WAT) is a key metabolic and endocrine organ regulating energy homeostasis, insulin sensitivity and inflammation, therefore functional WAT is essential in maintaining body homeostasis (Lafontan, 2014). There is strong evidence showing differences between subcutaneous adipose tissue (SAT) and visceral adipose tissue (VAT) biology, including distinct gene expression in VAT and SAT preadipocytes (Macotela et al., 2012; Tchkonia et al., 2013)

Animal models of PCOS are instrumental in dissecting mechanisms underlying the pathophysiology of PCOS (Abbott et al., 2013; Padmanabhan and Veiga-Lopez,

2013). We have previously documented that ewes exposed to increased androgens *in utero* manifest ovarian, hormonal and metabolic phenotypes reminiscent of PCOS (Hogg et al., 2011; 2012; Rae et al., 2013; Ramaswamy et al., 2016), and male offspring from such pregnancies display similar metabolic disturbances as seen in sons born to women with PCOS (Siemienowicz et al., 2019). We have reported that adult prenatally androgen-excess exposed (PA) sheep have increased body weight and are insulin resistant (Siemienowicz et al., 2020), while in adolescence those sheep are hyperinsulinemic and have increased fat accumulation in the liver, independent of body weight or central adiposity (Hogg et al., 2011). We hypothesised that the metabolic phenotype of PA sheep is associated with aberrant adipogenesis. Herein we investigate adipose tissue structure and function in adulthood and highlight aberrant adipogenesis in adolescence and its consequences in female PA sheep.

2. Materials and Methods

2.1 *Ethics statement*

All studies were approved by the UK Home Office and conducted under approved Project Licence PPL60/4401. The Animal Research Ethics Committee of The University of Edinburgh approved this study. The study was carried out in accordance with the relevant guidelines.

2.2 *Animals and tissues*

Animal husbandry, experimental protocols and tissue collection were performed as previously described (Hogg et al., 2012; 2011; Rae et al., 2013; Ramaswamy et al., 2016). Scottish Greyface ewes were housed in groups in spacious enclosures and fed hay *ad libitum*. Ewes with a healthy body condition score (2.75-3) were synchronised with Chronogest (flugestone) sponges (Intervet Ltd, UK) and Estrumate (cloprostenol) injection (Schering Plough Animal Health, UK) and mated with Texel rams. Pregnancy was suggested by lack of estrous and confirmed by ultrasound scanning.

In the maternal injection cohort (MI) pregnant ewes were randomised to twice weekly IM 100mg testosterone propionate (TP) in 1ml vegetable oil from day (D)62 to D102 of D147 pregnancy or 1ml vegetable oil (control (C)).

In pregnancies where fetal tissue was collected (D112: C=9; PA=4), ewes were sacrificed on D112 of gestation via barbiturate overdose. The gravid uterus was immediately removed, fetal sex and weight recorded, and tissue of interest snap frozen and stored at -80C.

In pregnancies carried to term, lambs were weaned at 3 months and fed hay or grass *ad libitum* until sacrifice at 11 weeks [juvenile (C=8; PA=8)]; 11 months, [adolescent (C=5; PA=9)] or 30 months [adult (C=11; PA=4)].

In the fetal injection cohort (FI), on day 62 and day 82 of gestation, mothers were randomised and anesthetised by initial sedation with 10 mg Xylazine (i.m. Rompun; Bayer PLC Animal Health Division, UK), followed by 2mg/kg Ketamine (i.v, Keteset; Fort Dodge Animal Health, UK). All subsequent procedures were conducted under surgical aseptic conditions. Fetuses were injected via ultrasound guidance into the fetal flank with 20G Quinke spinal needle (BD Biosciences, UK) with following according to the treatment group: control (C; n=12), 0.2ml vehicle (vegetable oil); testosterone propionate (TP; n=7), 20mg TP in 0.2ml vehicle; diethylsilbesterol (DES; n=8), 4mg DES in 0.2ml vehicle; dexamethasone (DEX; n=11), 100μg DEX in 0.2ml vehicle. Justification of the rationale, timing and treatment doses have been published previously (Siemienowicz et al., 2019). Immediately after surgical procedure completion all pregnant ewes were given prophylactic antibiotics (Streptacare, Animalcare Ltd., UK, 1 ml/25 kg) and were then monitored during recovery; no adverse effects of these procedures were observed. Lambs were weaned at 3 months and fed hay or grass ad libitum and sacrificed in adolescence (11 months of age).

Animals were sacrificed as described before (Hogg et al., 2011), omental tissue was carefully removed and weighed, and tissues of interest were fixed in Bouins solution for 24h, transferred to 70% ethanol and processed into paraffin wax and/or snap frozen and stored at -80C. Visceral adipose tissue was collected from omentum and subcutaneous adipose tissue from the groin area.

2.3 *Plasma analyte determination*

Concentrations of fasting plasma free fatty acids (FFAs), triglycerides (TGs), total cholesterol and high-density lipoprotein (HDL) were obtained using commercial assay kits (Alpha Laboratories Ltd., UK) as per manufacturer's instruction, using a

Cobas Mira automated analyser (Roche Diagnostics Ltd, UK). For all assays intra and inter-assay CV's were < 4% CV and < 5% CV, respectively. Fasting plasma leptin concentration was measured using Bio-Plex Human Diabetes Assay (171A7001M; Bio-Rad, UK), as per the manufacturer's instruction. All samples were assayed in duplicate and the results were acquired and calculated using Bio-Plex 200 array reader system with Bio-Plex Manager software (Bio-Rad, UK). The assay working range for leptin was 0.011-129ng/ml, assay sensitivity 3.1pg/ml, and intra and inter-assay CVs were 3% and 4%, respectively. Plasma adiponectin was measured using human Adiponectin ELISA kit (KHP041; Invitrogen, Life Technologies, UK), as per the manufacturer's instructions. All samples were assayed in duplicate. The assay sensitivity was 0.1ng/ml intra and inter-assay CVs were <5% and <6%, respectively.

2.4 *Adipocyte morphometric analysis*

For adipocyte morphometric analysis, two 5 μm sections were cut per adipose tissue sample, a minimum of 100 μm apart, and mounted on positively charged slides (Superfrost Plus Gold, Thermoscientific, UK). Sections were than stained with haematoxylin and eosin following standard protocol. Two randomly selected fields per section were captured at X4 magnification using Olympus Provis BX2 microscope (Olympus America Inc., USA) attached to a Canon EOS 30D Microcam camera (Canon Inc, Japan). Images were analysed using Adiposoft, ImageJ Software (Galarraga et al., 2012) in a blinded manner. Results were than manually corrected as per Adiposoft instructions and confirmed on a graticuled microscope.

2.5 *Western Blotting*

For western blotting all controls (C; n=5) and 5 samples from PA group were randomly selected for the analysis. Samples were homogenised with Soniprep150 (MSE UK

153 Ltd.) in RIPA buffer (ab156034, Abcam, UK) supplemented with HaltTM Protease
154 Inhibitor Cocktail (Thermo Scientific Pierce, USA) and centrifuged at 17500g at 4°C
155 for 10 min to pellet cellular debris. Protein concentration was measured using the
156 Bradford Assay on Cobas Fara centrifugal analyser (Roche Diagnostics, UK).
157 Samples were diluted in RIPA buffer and combined with equal volume of 1X Laemmli
158 buffer (0.1M Tris-HCl pH 6.8, 20% glycerol, 2% (w/v) SDS, 0.16% (w/v) bromophenol
159 blue and 3% β-mercaptoethanol). After heat denaturation (95^{o}C for 5 min), samples
160 (20 µg total protein) underwent electrophoresis, alongside full-range PageRulerTM
161 Plus Prestained Protein Ladder (Thermo Scientific Pierce, USA), on 4-20% Tris-
162 HEPES-SDS Precast Polyacrylamide Mini Gels (Thermo Scientific Pierce, USA) and
163 were transferred to a PVDF membrane (IPFL00010; Immobilon-FL PVDF; Merck
164 Millipore, Germany) using fast semi-dry blotter (Thermo Scientific Pierce, USA).
165 Membranes were blocked in Odyssey Blocking Buffer (Li-Cor, USA) overnight at 4°C.
166 Membrane was probed with primary antibody raised against STAT1 (1:1000; SC-346,
167 Santa Cruz Biotechnology) for 2h at RT, washed and probed with a primary antibody
168 raised against PPARγ (1:500; SC-1984 Santa Cruz Biotechnology) for 4h at RT. After
169 washing, membranes were incubated with two different fluorescently-labelled
170 secondary antibodies at the concentration 1:10000 IRDye 680RD (926-68074; Li-Cor)
171 and IRDye 800CW (926-32213; Li-Cor), both for 1h at RT. After final washing,
172 membranes were visualised on the Odyssey Imager (Li-Cor, USA). The size of the
173 visualised protein band was confirmed with reference to the molecular weight markers.
174 Protein densitometry was analysed with Image Studio Lite Software (Li-Cor, USA) with
175 STAT1 protein levels used as the loading control.

176 **2.5 *Quantitative (q)RT-PCR***

RNA was extracted from adipose tissue with a combination of TRI Reagent with the RNeasy Mini Kit (Qiagen Ltd.) and from liver using RNeasy Mini Kit following the manufacturer's instructions. On-column DNase digestion was performed using RNase-Free DNase set (Qiagen Ltd.) and RNA concentration and purity was assessed using a NanoDrop One spectrometer (ThermoFisher Scientific, UK). Complimentary DNA was synthesised using TaqMan Reverse Transcription Kit (Applied Biosystems, UK) as described previously (Hogg et al., 2012). To select the most stable housekeeping genes the geNorm Reference Gene Selection Kit (Primerdesign Ltd., UK) was used, identifying in visceral adipose tissue the suitability of the geometric mean of *RPS26* and *18S,* and for subcutaneous adipose tissue and liver the geometric mean of *ACTB* and *MDH1* was utilised.

Primers (Table 1) were designed and synthesised as described previously (Siemienowicz et al., 2020). Real time RT-PCR was performed on 384-well plate format (Applied Biosystems) with all samples assayed in duplicate and housekeeping control genes included in each run, as well as template, RNA and RT-negative controls, using the ABI 7900HT Fast Real Time PCR system (Applied Biosystems) as described previously (Hogg et al., 2012). The transcript abundance of target gene relative to the housekeeping genes was quantified using the $\Delta\Delta$Ct method (Livak and Schmittgen, 2001).

2.6 *Statistical analysis*

All data sets were normality tested prior to further analysis (Shapiro-Wilk test), and logarithmically transformed if necessary. For comparing means of two treatment groups with equal variances, unpaired, two-tailed Student's t test was used accepting $P<0.05$ as significant. For more than two comparisons ANOVA was used with Dunnett's post hoc test. Correlation was assessed by calculation of Pearson

product-moment co-efficient. Statistical analysis was performed using GraphPad Prism 8.0 software (GraphPad Prism Software, San Diego, CA, USA). Asterisks were used to indicate level of significance based on the following criteria: *P<0.05, **P<0.01.

3. Results

3.1 *PA sheep have structurally altered subcutaneous adipose tissue in adulthood*

Female PA sheep prenatally programmed to develop a PCOS-like condition show no difference in birth weight or body weight during the first year of life, through puberty and adolescence, however, in adulthood they have increased body weight as compared to controls (Siemienowicz et al., 2020). Adipocyte morphology was assessed by histological morphometric analysis (Fig. 1A). In VAT there was no difference in the numbers of adipocytes per mm^2 (Fig. 1B), no change in the mean size of adipocytes (Fig. 1C) and no alteration the number of adipocytes of different sizes (Fig. 1D). In contrast, adipocyte number was decreased in SAT (Fig. 1E; $P<0.05$), with a trend to an augmented mean size of adipocytes (Fig. 1F; $P=0.06$) as a result of an increased number of large adipocytes (defined as larger than 5000 μm^2) (Fig. 1G; $P<0.05$). The increased number of large SAT adipocytes in PA sheep was not a consequence of increased body weight as the difference was also observed between a weight-matched subset of controls (n=4) and PA sheep (n=4) (Fig. 1H; $P<0.05$). Key transcriptional regulators of adipogenesis, *PPARG*, *CEBPA*, *CEBPB* and *CEBPD* were not altered in adult VAT or SAT (Fig. 1I). There are fewer, but larger adipocytes in SAT in PA sheep but this was not associated with alterations in adipogenesis in adulthood.

3.2 *Prenatal androgen excess is associated with adipose tissue dysfunction in adulthood*

There were no differences in the transcript abundance of markers of mature adipocytes (*LEP* and *ADIPOQ*) in VAT or SAT (Fig. 2A) in adult PA sheep. Furthermore, there was no difference in plasma concentrations (Fig. 2B,C), although

there was a trend towards decreased adiponectin level (Fig. 2C; P=0.08) in PA sheep when compared to controls. There were no differences in transcript abundance of inflammatory markers in VAT (Fig. 2D) while in SAT PA sheep had increased *TNF* (P<0.05), *IL6* (P<0.05) and *CCL2* (P<0.05) when compared to controls (Fig. 2E; P<0.05). Although the PA sheep have normal levels of TGs, cholesterol and HDL cholesterol (Fig. 3A-C) they have increased circulating FFAs (Fig. 3D; P<0.05). There was negative correlation (r= -0.66) between the total number of adipocytes per mm^2 and the levels of circulating FFAs (Fig. 3E; P<0.05). Although at this time there was no difference in omental fat (Fig. 3F) there was increased transcript abundance of genes involved in fat uptake and accumulation in VAT (*SLC27A1*, *CAV1*, *CAV2, FABP5 and LPIN2*) (Fig. 3G-K; P<0.05). Alterations in adipose tissue associated with inflammation is seen in SAT only and this is associated with increased FFAs. In summary, we observed structurally altered subcutaneous adipose tissue, with attendant dysfunction in adulthood attributable to prenatal androgen excess.

3.3 *Altered adipogenesis is observed during adolescence*

We next assessed expression of transcription factors involved in adipogenesis at 11 months of age when there was no difference in body weight (Siemienowicz et al., 2020) and omental fat weight (Hogg et al., 2011). In VAT there was no difference in the transcript abundance of *PPARG*, *CEBPA and CEBPB,* although *CEBPD* was increased (P<0.05) in adolescent PA sheep (Fig. 4A). However, in SAT there was decreased transcript abundance of *PPARG*, *CEBPA, CEBPB* (Fig. 4B; P<0.05) but no difference in *CEBPD* (Fig. 4B). We confirmed decreased level of PPARG in SAT (Fig. 4C; P<0.05) in adolescent PA females, by Western blot. In addition, adolescent PA sheep had decreased expression of markers of mature adipocytes in SAT,

257 *SLC2A4* and *PLIN1* (Supplementary Figure 1; P<0.05-0.01). In order to determine
258 the specificity of prenatal androgens in the regulation of adolescent adipogenesis
259 (Fig. 4D) we directly injected various steroids into the mid-gestation fetus and
260 assessed adipogenesis markers in SAT in adolescence. Reduced adipogenesis-
261 associated gene expression in SAT was only associated with prenatal androgen
262 excess (TP) and neither estrogenic (DES) excess nor glucocorticoid (DEX) excess
263 showed similar effects (Fig. 4D; P<0.05).

264 **3.4 *Adolescent SAT transcriptional alterations are associated with increased***
265 ***circulating FFA***

266 Fasting FFAs were increased in adolescent PA sheep when compared to controls
267 (Fig. 5A; P<0.05). Their concentrations were negatively correlated with *PPARG* (r=-
268 0.55) in SAT (Fig. 5B; P<0.05) but not with *PPARG* in VAT (Fig. 5C). These sheep
269 have early accumulation of fat in the liver (Hogg et al., 2011) with increased
270 transcript abundance of genes involved in FFAs uptake and deposition in the liver
271 (Fig. 5D-F; P<0.05).

272 **3.5 *Adiponectin is a biomarker of reduced SAT adipogenesis during***
273 ***adolescence***

274 To investigate potential biomarkers of altered adipogenesis during adolescence the
275 transcript abundance of markers of mature adipocytes was investigated in adipose
276 tissue at 11 months of age in control and PA animals. In VAT there was no changes
277 in *LEP* or *ADIPOQ* expression (Fig. 6A,B). In contrast *LEP* (P<0.01) and *ADIPOQ*
278 (P<0.05) were reduced in SAT in adolescent PA sheep when compared to controls
279 (Fig. 6C,D). This was reflected by a reduction in circulating leptin (Fig 6E; P<0.05)
280 and adiponectin (Fig. 6F; P<0.05) in the plasma. Circulating adiponectin correlated
281 (r=0.79) to *ADIPOQ* in SAT (Fig. 6G; P<0.01) but not VAT (Fig. 6H), and there was

282 no correlation identified between circulating leptin and SAT *LEP* gene expression.
283 Collectively, in female PA offspring, we observed altered adipogenesis during
284 adolescence, with increased circulating FFA, and this response was specific to
285 androgenic excess during development. Reduced circulating adiponectin has
286 potential as a biomarker of reduced adipogenesis in SAT during adolescence.
287 **3.6 *There is no evidence of altered adipogenesis before puberty***
288 Altered transcript abundance for transcription factors involved in adipogenesis was
289 not observed pre-pubertally at 11 weeks of age or in fetal life (Table 1).
290

4. Discussion

We demonstrated, using an ovine model of PCOS, that during adolescence, but not fetal or prepubertal life, there was decreased adipogenesis in SAT in PA sheep. This was accompanied by decreased concentrations of leptin and adiponectin, and increased concentrations of FFAs, likely underpinning the observation of upregulated expression of FFAs transporters in liver. Adult consequences of such altered adolescent adipogenesis were that PA female offspring displayed adipocyte hypertrophy in SAT paralleled by increased expression of inflammatory markers and increased expression of genes linked to fat accumulation in VAT.

In fetal life pre-adipocyte differentiation into adipocytes occurs between the 14th and the 16th weeks of gestation in humans (Poissonnet et al., 1983) and in the third month of gestation in sheep (Wensvoort, 1967). In late gestation adipocyte proliferation decreases, and until adolescence, increased adiposity primarily occurs via filling of predetermined adipocytes. During puberty another window of adipocyte proliferation occurs (Rosen and Spiegelman, 2014) setting the total number of adipocytes. Whilst differentiation potential of pre-adipocytes into mature adipocytes is present throughout life, dependent upon energy status and storage needs (Rosen and Spiegelman, 2014), in adult life, the capacity of preadipocytes to become fully functional mature adipocytes declines (Tchkonia et al., 2010). Hence increased or decreased adult body weight, with corresponding fluctuations in body fat mass, is reflective of changes in adipocyte volume but not number (MacLean et al., 2015; Spalding et al., 2008). In our study altered adipogenesis in SAT of PA females was only evident during adolescence (11 months).

316 During adipogenesis, pre-adipocyte terminal differentiation to mature adipocytes
317 involves accruing lipid transport and synthesis capacity, insulin responsiveness and
318 synthesis of adipokines, regulated by PPARG and the family of CCAAT/enhancer
319 binding protein transcription factors (C/EBP) (Cristancho and Lazar, 2011). SAT
320 expansion improves lipid buffering and metabolic profile (Kim et al., 2007) while
321 inability to increase adipose cell number results in hypertrophic adipocytes,
322 increasing risk of metabolic diseases (Dubois et al., 2006). Impaired SAT
323 adipogenesis results in decreased storage capacity, and accumulation of lipids in
324 non-adipose tissues, lipotoxicity and metabolic perturbations (Carobbio et al., 2017).
325 Furthermore, decreased subcutaneous pre-adipocyte differentiation and defective
326 storage capacity of SAT are associated with increased visceral adiposity (Alligier et
327 al., 2013; Lessard et al., 2014), suggesting increased visceral fat accumulation might
328 be a compensatory adaptation to limitations in SAT expandability (Britton and Fox,
329 2011).
330
331 Decreased expression of PPARG, *CEBPA* and *CEBPB* in SAT, in PA sheep
332 suggests decreased differentiation of pre-adipocytes into mature adipocytes and
333 indicates lower capacity of SAT to safely store fat, which combined with observations
334 of increased levels of FFAs in PA adolescent sheep supports suggestions of
335 decreased lipid storage volume in SAT. This may also contribute to fatty liver
336 development due to increased release of FFAs into circulation and increased hepatic
337 uptake (Hogg et al., 2011). Morphometric analysis of the SAT in adolescent sheep
338 was not performed due to lack of histological samples, as the aim of the study was to
339 determine adult outcomes in terms of adipose structure, and examine the earlier life
340 mechanistic antecedents of any altered adult structure observed; we acknowledge

this limitation of the data presented here. Veiga-Lopez *et al*. previously reported that postpubertal, (21 months old), prenatally androgenised female sheep showed reduction in adipocyte cell size in both VAT and SAT and concluded failure of a subset of small adipocytes to differentiate. (Veiga-Lopez et al., 2013). We did not observe any effect on VAT in our adolescent animals. The discrepancies between studies may be attributed to different timing of the prenatal testosterone treatment and different age at study.

Adipogenesis in PCOS patients has not been thoroughly investigated, however, increased abdominal adipose stem cell commitment to preadipocytes *in vitro*, as measured by the expression of ZFP423 protein, have been found in adult, normal weight women with PCOS (Fisch et al., 2018). Increased *ZFP423* gene expression was also reported in abdominal SAT of prenatally androgenised female rhesus monkeys (Keller et al., 2014). We did not study the preadipocyte commitment but rather, the differentiation of preadipocytes into mature adipocytes. In agreement with our study, it was reported that women with PCOS have decreased expression and increased DNA methylation of *PPARG* in SAT and *PPARG* expression positively correlated with insulin sensitivity and negatively with adipocyte size and testosterone levels (Kokosar et al., 2016). Furthermore, PCOS-like monkeys were also have decreased abdominal SAT *CEBPA* expression, reduced numbers of mature SAT adipocytes and increased FFAs indicating impaired adipogenesis (Keller et al., 2014). In addition, there is growing evidence of decreased adipogenesis in SAT from insulin resistant individuals and subjects with abdominal obesity (Heilbronn et al., 2004; Permana et al., 2004; Yang et al., 2004). Our data is in broad agreement with such observations, lending translational confidence to our findings.

Further translational relevance in terms of PCOS is derived from observations that obese adolescent girls with PCOS have persistently elevated FFAs when compared with obese controls (King et al., 2017). Since SAT represents approximately 80% of total body adipose tissue, decreased SAT adipogenesis in adolescence may predispose to decreased storage capacity in adulthood and increased adipocyte hypertrophy. In support of this, our adult PA sheep have decreased SAT adipocyte numbers and corresponding increased numbers of large, hypertrophic adipocytes, and adult PCOS women have hypertrophic adipocytes in SAT (Echiburú et al., 2018; Faulds et al., 2003; Manneras-Holm et al., 2010).

Hypertrophic expansion of SAT is associated with altered adipokine secretion, inflammation and fibrosis (Longo et al., 2019). Adipocyte hypertrophy in adult PA sheep was paralleled by increased expression of *TNF*, *IL6* and *CCL2* in SAT. Enlarged adipocytes overexpress MCP-1 (encoded by *CCL2* gene) and induce increased recruitment of proinflammatory M1 macrophages culminating in increased production of pro-inflammatory cytokines TNFα and IL-6, promoting altered gene expression and insulin resistance in adipocytes (Weisberg et al., 2003).

Adolescent PA sheep had also decreased expression of markers of mature adipocytes *LEP* and *ADIPOQ* in SAT, functionally realised by decreased circulating leptin and adiponectin concentrations. There was positive correlation of *ADIPOQ* mRNA in SAT, with circulating adiponectin, reminiscent of that observed in women with PCOS (Echiburú et al., 2018; Lecke et al., 2013), and suggesting the likelihood that decreased adiponectin levels in adolescent PCOS-like sheep is a consequence of decreased adipogenesis in SAT. Adiponectin, primarily secreted from SAT, is an

391 insulin sensitising adipokine, promoting lipid oxidation and reducing plasma
392 concentration of FFAs (Achari and Jain, 2017), and stimulates glucose uptake in
393 adipocytes by increasing expression of GLUT4 (Achari and Jain, 2017; Fu et al.,
394 2005).
395
396 Adiponectin is also an autocrine factor promoting and regulating adipocyte
397 differentiation (do Carmo Avides et al., 2008; Fu et al., 2005). Decreased circulating
398 adiponectin levels, independent of adiposity, are consistently reported in adolescent
399 and adult PCOS patients (Cankaya et al., 2014; Escobar-Morreale et al., 2006;
400 Maliqueo et al., 2012; Mirza et al., 2014; Sepilian and Nagamani, 2005), suggesting
401 potential utility as a biomarker of PCOS (Al-Awadi et al., 2016; Sarray et al., 2015).
402 Whilst androgens decrease plasma adiponectin *in vitro* and *in vivo* (Frederiksen et
403 al., 2012; Nishizawa et al., 2002; Xu et al., 2005), and this is inversely correlated with
404 testosterone levels, (Böttner et al., 2004; Riestra et al., 2013), to our knowledge this
405 is the first demonstration of prenatal androgen excess being associated with
406 decreased SAT and circulating adiponectin. It is noteworthy in the context of prenatal
407 androgenic programming of PCOS that adiponectin decreases ovarian thecal
408 androgen synthesis and expression of adiponectin receptors is decreased in theca
409 cells from polycystic ovaries; consequently decreased adiponectin may also
410 contribute to hyperandrogenism in PCOS women (Comim et al., 2013; Lagaly et al.,
411 2008).
412
413 Inhibitory effects of androgens on adipogenesis is well documented (Zerradi et al.,
414 2014). Numerous studies demonstrate androgens prevent *in vitro* differentiation and
415 proliferation of murine preadipocyte cell lines (Fujioka et al., 2012; Singh et al., 2003;

2005) and human preadipocytes from both sexes, and from different fat depots (Blouin et al., 2010; Chazenbalk et al., 2013; Gupta et al., 2008; McNelis et al., 2013). To determine steroid specificity of androgenic excess in programming adipose tissue function *in vivo*, we assessed SAT adipogenesis in adolescent, 11 months old female sheep, that were directly injected *in utero* with androgen, estrogen (DES as surrogate estrogen) or glucocorticoid (DEX as surrogate, active glucocorticoid). We found that only androgen treatment, but not estrogen or glucocorticoid, decreased adipogenesis in SAT in adolescence, identifying that the responses measured throughout the study were androgenic.

In summary, we have shown that during adolescence, altered adipogenesis in SAT of PA sheep occurs, with decreased beneficial adipokines, independent of central adiposity. Decreased adipocyte differentiation during adolescence resulted in hypertrophy and inflammation of adult SAT. This decreased capacity of SAT to safely store fat may explain metabolic perturbations observed in PA female sheep, shedding light upon new investigatory, and interventional avenues in clinical PCOS research.

Acknowledgements

The authors wish to acknowledge Joan Docherty, John Hogg, Marjorie Thomson, Peter Tennant and James Nixon and the staff at the Marshall Building, University of Edinburgh for their excellent animal husbandry. Dr Kirsten Hogg, Dr Fiona Connolly, Dr Junko Nio-Kobayashi, Dr Avi Lerner and Lyndsey Boswell helped with tissue collection.

Funding

This work was funded by Medical Research Council (MRC) project grants (G0500717; G0801807; G0802782; MR/P011535/1) and supported by the MRC Centre for Reproductive Health (MR/N022556/1).

Declaration of interest

The authors have no conflicts of interest to declare.

References

Abbott, D.H., Nicol, L.E., Levine, J.E., Xu, N., Goodarzi, M.O., Dumesic, D.A., 2013. Nonhuman primate models of polycystic ovary syndrome. Mol. Cell. Endocrinol. 373, 21–28. doi:10.1016/j.mce.2013.01.013

Achari, A.E., Jain, S.K., 2017. Adiponectin, a Therapeutic Target for Obesity, Diabetes, and Endothelial Dysfunction. Int. J. Mol. Sci. 18, 1321. doi:10.3390/ijms18061321

Al-Awadi, A.M., Sarray, S., Arekat, M.R., Saleh, L.R., Mahmood, N., Almawi, W.Y., 2016. The high-molecular weight multimer form of adiponectin is a useful marker of polycystic ovary syndrome in Bahraini Arab women. Clin. Nutr. ESPEN 13, e33–e38. doi:10.1016/j.clnesp.2016.03.078

Alligier, M., Gabert, L., Meugnier, E., Lambert-Porcheron, S., Chanseaume, E., Pilleul, F., Debard, C., Sauvinet, V., Morio, B., Vidal-Puig, A., Vidal, H., Laville, M., 2013. Visceral fat accumulation during lipid overfeeding is related to subcutaneous adipose tissue characteristics in healthy men. J. Clin. Endocrinol. Metab. 98, 802–810. doi:10.1210/jc.2012-3289

Blouin, K., Nadeau, M., Perreault, M., Veilleux, A., Drolet, R., Marceau, P., Mailloux, J., Luu-The, V., Tchernof, A., 2010. Effects of androgens on adipocyte differentiation and adipose tissue explant metabolism in men and women. Clin. Endocrinol. 72, 176–188. doi:10.1111/j.1365-2265.2009.03645.x

473 Böttner, A., Kratzsch, J., Müller, G., Kapellen, T.M., Blüher, S., Keller, E., Blüher, M.,
474 Kiess, W., 2004. Gender Differences of Adiponectin Levels Develop during the
475 Progression of Puberty and Are Related to Serum Androgen Levels. J. Clin.
476 Endocrinol. Metab. 89, 4053–4061. doi:10.1210/jc.2004-0303
477
478 Britton, K.A., Fox, C.S., 2011. Ectopic Fat Depots and Cardiovascular Disease.
479 Circulation 124, e837-41. doi:10.1161/CIRCULATIONAHA.111.077602
480
481 Cankaya, S., Demir, B., Aksakal, S.E., Dilbaz, B., Demirtas, C., Goktolga, U., 2014.
482 Insulin resistance and its relationship with high molecule weight adiponectin in
483 adolescents with polycystic ovary syndrome and a maternal history. Fertil. Steril.
484 102, 826–830. doi:10.1016/j.fertnstert.2014.05.032
485
486 Carmina, E., Orio, F., Palomba, S., Cascella, T., Longo, R.A., Colao, A.M.,
487 Lombardi, G., Lobo, R.A., 2005. Evidence for altered adipocyte function in polycystic
488 ovary syndrome. Eur. J. Endocrinol. 152, 389–394. doi:10.1530/eje.1.01868
489
490 Carobbio, S., Pellegrinelli, V., Vidal-Puig, A., 2017. Adipose Tissue Function and
491 Expandability as Determinants of Lipotoxicity and the Metabolic Syndrome. Adv.
492 Exp. Med. Biol. 960, 161–196. doi:10.1007/978-3-319-48382-5_7
493
494 Chazenbalk, G., Singh, P., Irge, D., Shah, A., Abbott, D.H., Dumesic, D.A., 2013.
495 Androgens inhibit adipogenesis during human adipose stem cell commitment to
496 preadipocyte formation. Steroids 78, 920–926. doi:10.1016/j.steroids.2013.05.001

Comim, F.V., Hardy, K., Franks, S., 2013. Adiponectin and Its Receptors in the Ovary: Further Evidence for a Link between Obesity and Hyperandrogenism in Polycystic Ovary Syndrome. PLoS ONE 8, e80416. doi:10.1371/journal.pone.0080416

Cristancho, A.G., Lazar, M.A., 2011. Forming functional fat: a growing understanding of adipocyte differentiation. Nat. Rev. Mol. Cell Biol. 12, 722–734. doi:10.1038/nrm3198

do Carmo Avides, M., Domingues, L., Vicente, A., Teixeira, J., 2008. Differentiation of human pre-adipocytes by recombinant adiponectin. Protein Expr. Purif. 59, 122–126. doi:10.1016/j.pep.2008.01.012

Dubois, S.G., Heilbronn, L.K., Smith, S.R., Albu, J.B., Kelley, D.E., Ravussin, E., Look AHEAD Adipose Research Group, 2006. Decreased expression of adipogenic genes in obese subjects with type 2 diabetes. Obesity 14, 1543–1552. doi:10.1038/oby.2006.178

Echiburú, B., Pérez-Bravo, F., Galgani, J.E., Sandoval, D., Saldías, C., Crisosto, N., Maliqueo, M., Sir-Petermann, T., 2018. Enlarged adipocytes in subcutaneous adipose tissue associated to hyperandrogenism and visceral adipose tissue volume in women with polycystic ovary syndrome. Steroids 130, 15–21. doi:10.1016/j.steroids.2017.12.009

521 Escobar-Morreale, H.F., Villuendas, G., Botella-Carretero, J.I., Álvarez-Blasco, F.,
522 Sanchón, R., Luque-Ramírez, M., Millán, J.L.S., 2006. Adiponectin and resistin in
523 PCOS: a clinical, biochemical and molecular genetic study. Hum. Reprod. 21, 2257–
524 2265. doi:10.1093/humrep/del146
525
526 Faulds, G., Ryden, M., Ek, I., 2003. Mechanisms behind lipolytic catecholamine
527 resistance of subcutaneous fat cells in the polycystic ovarian syndrome. J. Clin.
528 Endocrinol. Metab. 88, 2269. doi:10.1210/jc.2002-021573
529
530 Fauser BCJM, Tarlatzis BC, Rebar RW, Legro RS, Balen AH, Lobo R, Carmina E,
531 Chang J, Yildiz BO, Laven JSE *et al.* 2012 Consensus on women's health aspects of
532 polycystic ovary syndrome (PCOS): the Amsterdam ESHRE/ASRM-Sponsored 3rd
533 PCOS Consensus Workshop Group. Hum. Reprod. 27, 14-24. doi:
534 10.1093/humrep/der396
535
536 Fisch, S.C., Nikou, A.F., Wright, E.A., Phan, J.D., Leung, K.L., Grogan, T.R., Abbott,
537 D.H., Chazenbalk, G.D., Dumesic, D.A., 2018. Precocious subcutaneous abdominal
538 stem cell development to adipocytes in normal-weight women with polycystic ovary
539 syndrome. Fertil. Steril. 110, 1367–1376. doi:10.1016/j.fertnstert.2018.08.042
540
541 Frederiksen, L., Højlund, K., Hougaard, D.M., Mosbech, T.H., Larsen, R., Flyvbjerg,
542 A., Frystyk, J., Brixen, K., Andersen, M., 2012. Testosterone therapy decreases
543 subcutaneous fat and adiponectin in aging men. Eur. J. Endocrinol. 166, 469–476.
544 doi:10.1530/EJE-11-0565
545

546 Fu, Y., Luo, N., Klein, R.L., Garvey, W.T., 2005. Adiponectin promotes adipocyte
547 differentiation, insulin sensitivity, and lipid accumulation. J. Lipid Res. 46, 1369–
548 1379. doi:10.1194/jlr.M400373-JLR200
549
550 Fujioka, K., Fujioka, K., Kajita, K., Kajita, K., WU, Z., Hanamoto, T., Wu, Z.,
551 Hanamoto, T., Ikeda, T., Ikeda, T., Mori, I., Okada, H., Mori, I., Okada, H., Yamauchi,
552 M., Yamauchi, M., Uno, Y., Morita, H., Uno, Y., Nagano, I., Morita, H., Takahashi, Y.,
553 Nagano, I., Takahashi, Y., Ishizuka, T., Ishizuka, T., 2012. Dehydroepiandrosterone
554 reduces preadipocyte proliferation via androgen receptor. Am. J. Physiol. Endocrinol.
555 Metab. 302, E694–704. doi:10.1152/ajpendo.00112.2011
556
557 Galarraga, M., Campión, J., Muñoz-Barrutia, A., Boqué, N., Moreno, H., Martínez,
558 J.A., Milagro, F., Ortiz-de-Solórzano, C., 2012. Adiposoft: automated software for the
559 analysis of white adipose tissue cellularity in histological sections. J. Lipid Res. 53,
560 2791–2796. doi:10.1194/jlr.D023788
561
562 Gupta, V., Bhasin, S., Guo, W., Singh, R., Miki, R., Chauhan, P., Choong, K.,
563 Tchkonia, T., Lebrasseur, N.K., Flanagan, J.N., Hamilton, J.A., Viereck, J.C., Narula,
564 N.S., Kirkland, J.L., Jasuja, R., 2008. Effects of dihydrotestosterone on differentiation
565 and proliferation of human mesenchymal stem cells and preadipocytes. Mol. Cell.
566 Endocrinol. 296, 32–40. doi:10.1016/j.mce.2008.08.019
567
568 Heilbronn, L., Smith, S.R., Ravussin, E., 2004. Failure of fat cell proliferation,
569 mitochondrial function and fat oxidation results in ectopic fat storage, insulin

570 resistance and type II diabetes mellitus. Int. J. Obes. 28, S12–S21.
571 doi:10.1038/sj.ijo.0802853
572
573 Hogg, K., Wood, C., McNeilly, A.S., Duncan, W.C., 2011. The in utero programming
574 effect of increased maternal androgens and a direct fetal intervention on liver and
575 metabolic function in adult sheep. PLoS ONE 6, e24877.
576 doi:10.1371/journal.pone.0024877
577
578 Hogg, K., Young, J.M., Oliver, E.M., Souza, C.J., McNeilly, A.S., Duncan, W.C.,
579 2012. Enhanced Thecal Androgen Production Is Prenatally Programmed in an Ovine
580 Model of Polycystic Ovary Syndrome. Endocrinology 153, 450–461.
581 doi:10.1210/en.2011-1607
582
583 Jason, J., 2011. Polycystic ovary syndrome in the United States: clinical visit rates,
584 characteristics, and associated health care costs. Arch. Intern. Med. 171, 1209–
585 1211. doi:10.1001/archinternmed.2011.288
586
587 Keller, E., Chazenbalk, G.D., Aguilera, P., Madrigal, V., Elashoff, D., Grogan, T.,
588 Dumesic, D.A., Abbott, D.H., 2014. Impaired preadipocyte differentiation into
589 adipocytes in subcutaneous abdominal adipose of PCOS-like female rhesus
590 monkeys. Endocrinology 155, 2696–2703. doi:10.1210/en.2014-1050
591
592 Kim, J.-Y., van de Wall, E., Laplante, M., Azzara, A., Trujillo, M.E., Hofmann, S.M.,
593 Schraw, T., Durand, J.L., Li, H., Li, G., Jelicks, L.A., Mehler, M.F., Hui, D.Y.,
594 Deshaies, Y., Shulman, G.I., Schwartz, G.J., Scherer, P.E., 2007. Obesity-

595 associated improvements in metabolic profile through expansion of adipose tissue. J.
596 Clin. Invest. 117, 2621–2637. doi:10.1172/JCI31021
597
598 King, M., Dorosz, J., Patel, S.S., Kinney, G.L., Cree-Green, M., Wang, H., Ferland,
599 A., Truong, U., Nadeau, K.J., Maahs, D.M., Eckel, R.H., Moreau, K.L., Hokanson,
600 J.E., 2017. Obese adolescents with polycystic ovarian syndrome have elevated
601 cardiovascular disease risk markers. Vasc. Med. 22, 85–95.
602 doi:10.1177/1358863X16682107
603
604 Klemm, D.J., Leitner, J.W., Watson, P., Nesterova, A., Reusch, J., Goalstone, M.L.,
605 Draznin, B., 2001. Insulin-induced adipocyte differentiation - Activation of CREB
606 rescues adipogenesis from the arrest caused by inhibition of prenylation. J. Biol.
607 Chem. 276, 28430–28435. doi:10.1074/jbc.m103382200
608
609 Kokosar, M., Benrick, A., Perfilyev, A., Fornes, R., Nilsson, E., Maliqueo, M., Behre,
610 C.J., Sazonova, A., Ohlsson, C., Ling, C., Stener-Victorin, E., 2016. Epigenetic and
611 Transcriptional Alterations in Human Adipose Tissue of Polycystic Ovary Syndrome
612 SCI. Rep. 6, 22883. doi:10.1038/srep22883
613
614 Lafontan, M., 2014. Adipose tissue and adipocyte dysregulation. Diabetes Metab.
615 40, 16–28. doi:10.1016/j.diabet.2013.08.002
616
617 Lagaly, D.V., Aad, P.Y., Grado-Ahuir, J.A., Hulsey, L.B., Spicer, L.J., 2008. Role of
618 adiponectin in regulating ovarian theca and granulosa cell function. Mol. Cell.
619 Endocrinol. 284, 38–45. doi:10.1016/j.mce.2008.01.007

Lecke, S.B., Morsch, D.M., Spritzer, P.M., 2013. Association between adipose tissue expression and serum levels of leptin and adiponectin in women with polycystic ovary syndrome. Genet. Mol. Res. 12, 4292–4296. doi:10.4238/2013.February.28.16

Lessard, J., Laforest, S., Pelletier, M., Leboeuf, M., Blackburn, L., Tchernof, A., 2014. Low abdominal subcutaneous preadipocyte adipogenesis is associated with visceral obesity, visceral adipocyte hypertrophy, and a dysmetabolic state. Adipocyte 3, 197–205. doi:10.4161/adip.29385

Livak, K.J., Schmittgen, T.D., 2001. Analysis of Relative Gene Expression Data Using Real-Time Quantitative PCR and the 2−ΔΔCT Method. Methods 25, 402–408. doi:10.1006/meth.2001.1262

Longo, M., Zatterale, F., Naderi, J., Parrillo, L., Formisano, P., Raciti, G.A., Beguinot, F., Miele, C., 2019. Adipose Tissue Dysfunction as Determinant of Obesity-Associated Metabolic Complications. Int. J. Mol. Sci. 20, 2358. doi:10.3390/ijms20092358

MacLean, P.S., Higgins, J.A., Giles, E.D., Sherk, V.D., Jackman, M.R., 2015. The role for adipose tissue in weight regain after weight loss. Obes. Rev. 16, 45–54. doi:10.1111/obr.12255

Macotela, Y., Emanuelli, B., Mori, M.A., Gesta, S., 2012. Intrinsic differences in adipocyte precursor cells from different white fat depots. Diabetes 61, 1691–1699. doi:10.2337/db11-1753

Maliqueo, M., Maliqueo, M., Pérez-Bravo, F., Galgani, J.E., Galgani, J.E., Pérez, F., Echiburú, B., Echiburú, B., Crisosto, N., de Guevara, A.L., Sir-Petermann, T., 2012. Relationship of serum adipocyte-derived proteins with insulin sensitivity and reproductive features in pre-pubertal and pubertal daughters of polycystic ovary syndrome women. Eur. J. Obstet. Gynecol. Reprod. Biol. 161, 56–61. doi:10.1016/j.ejogrb.2011.12.012

Manneras-Holm, L., Leonhardt, H., Jennische, E., Kullberg, J., Oden, A., Holm, G., Hellstrom, M., Lonn, L., Olivecrona, G., Stener-Victorin, E., Lonn, M., 2010. Adipose tissue has aberrant morphology and function in PCOS: enlarged adipocytes and low serum adiponectin, but not circulating sex steroids, are strongly associated with insulin resistance. J. Clin. Endocrinol. Metab. 96, E304–11. doi:10.1210/jc.2010-1290

McNelis, J.C., Manolopoulos, K.N., Gathercole, L.L., Bujalska, I.J., Stewart, P.M., Tomlinson, J.W., Arlt, W., 2013. Dehydroepiandrosterone exerts antiglucocorticoid action on human preadipocyte proliferation, differentiation, and glucose uptake. Am. J. Physiol. Endocrinol. Metab. 305, E1134–44. doi:10.1152/ajpendo.00314.2012

Mirza, S.S., Shafique, K., Shaikh, A.R., Khan, N.A., Anwar Qureshi, M., Qureshi, M.A., 2014. Association between circulating adiponectin levels and polycystic ovarian syndrome. J. Ovarian Res. 7, 18. doi:10.1186/1757-2215-7-18

668 Moran, L.J., Teede, H.J., Norman, R.J., 2015. Metabolic risk in PCOS: phenotype
669 and adiposity impact. Trends Endocrinol. Metab. 26, 136–143.
670 doi:10.1016/j.tem.2014.12.003
671
672 Nishizawa, H., Shimomura, I., Kishida, K., Maeda, N., Kuriyama, H., Nagaretani, H.,
673 Matsuda, M., Kondo, H., Furuyama, N., Kihara, S., Nakamura, T., Tochino, Y.,
674 Funahashi, T., Matsuzawa, Y., 2002. Androgens decrease plasma adiponectin, an
675 insulin-sensitizing adipocyte-derived protein. Diabetes 51, 2734–2741.
676
677 Padmanabhan, V., Veiga-Lopez, A., 2013. Sheep models of polycystic ovary
678 syndrome phenotype. Mol. Cell. Endocrinol. 373, 8–20.
679 doi:10.1016/j.mce.2012.10.005
680
681 Permana, P.A., Nair, S., Lee, Y.-H., Luczy-Bachman, G., Vozarova De Courten, B.,
682 Tataranni, P.A., 2004. Subcutaneous abdominal preadipocyte differentiation in vitro
683 inversely correlates with central obesity. Am. J. Physiol. Endocrinol. Metab. 286,
684 E958–62. doi:10.1152/ajpendo.00544.2003
685
686 Poissonnet, C.M., Burdi, A.R., Bookstein, F.L., 1983. Growth and development of
687 human adipose tissue during early gestation. Early Hum. Dev. 8, 1–11.
688 doi:10.1016/0378-3782(83)90028-2
689
690 Puder, J.J., Varga, S., Kraenzlin, M., De Geyter, C., Keller, U., Müller, B., 2005.
691 Central fat excess in polycystic ovary syndrome: relation to low-grade inflammation

692 and insulin resistance. J. Clin. Endocrinol. Metab. 90, 6014–6021.
693 doi:10.1210/jc.2005-1002
694
695 Puttabyatappa, M., Lu, C., Martin, J.D., Chazenbalk, G., Dumesic, D.,
696 Padmanabhan, V., 2018. Developmental Programming: Impact of Prenatal
697 Testosterone Excess on Steroidal Machinery and Cell Differentiation Markers in
698 Visceral Adipocytes of Female Sheep. Reprod. Sci. 25, 1010–1023.
699 doi:10.1177/1933719117746767
700
701 Rae, M., Grace, C., Hogg, K., Wilson, L.M., McHaffie, S.L., Ramaswamy, S.,
702 MacCallum, J., Connolly, F., McNeilly, A.S., Duncan, C., 2013. The pancreas is
703 altered by in utero androgen exposure: implications for clinical conditions such as
704 polycystic ovary syndrome (PCOS). PLoS ONE 8, e56263.
705 doi:10.1371/journal.pone.0056263
706
707 Ramaswamy, S., Grace, C., Mattei, A.A., Siemienowicz, K., Brownlee, W.,
708 MacCallum, J., McNeilly, A.S., Duncan, W.C., Rae, M.T., 2016. Developmental
709 programming of polycystic ovary syndrome (PCOS): prenatal androgens establish
710 pancreatic islet α/β cell ratio and subsequent insulin secretion. Sci. Rep. 6, 27408.
711 doi:10.1038/srep27408
712
713 Riestra, P., Garcia-Anguita, A., Ortega, L., Garces, C., 2013. Relationship of
714 Adiponectin with Sex Hormone Levels in Adolescents. Horm. Res. Paediatr. 79, 83–
715 87. doi:10.1159/000346898
716

717 Rosen, E.D., Spiegelman, B.M., 2014. What We Talk About When We Talk About
718 Fat. Cell 156, 20–44. doi:10.1016/j.cell.2013.12.012
719
720 Sarray, S., Madan, S., Saleh, L.R., Mahmoud, N., Almawi, W.Y., 2015. Validity of
721 adiponectin-to-leptin and adiponectin-to-resistin ratios as predictors of polycystic
722 ovary syndrome. Fertil. Steril. 104, 460–466. doi:10.1016/j.fertnstert.2015.05.007
723
724 Seow, K.-M., Tsai, Y.-L., Hwang, J.-L., Hsu, W.-Y., Ho, L.-T., Juan, C.-C., 2009.
725 Omental adipose tissue overexpression of fatty acid transporter CD36 and
726 decreased expression of hormone-sensitive lipase in insulin-resistant women with
727 polycystic ovary syndrome. Hum. Reprod. 24, 1982–1988.
728 doi:10.1093/humrep/dep122
729
730 Sepilian, V., Nagamani, M., 2005. Adiponectin levels in women with polycystic ovary
731 syndrome and severe insulin resistance. J. Soc. Gynecol. Invest. 12, 129–134.
732 doi:10.1016/j.jsgi.2004.09.003
733
734 Siemienowicz, K., Rae, M.T., Howells, F., Anderson, C., Nicol, L.M., Franks, S.,
735 Duncan, W.C., 2020. Insights into manipulating postprandial energy expenditure to
736 manage weight gain in polycystic ovary syndrome (PCOS). iScience 101164.
737 doi:10.1016/j.isci.2020.101164
738
739 Siemienowicz, K.J., Filis, P., Shaw, S., Douglas, A., Thomas, J., Mulroy, S., Howie,
740 F., Fowler, P.A., Duncan, W.C., Rae, M.T., 2019. Fetal androgen exposure is a

741 determinant of adult male metabolic health. Sci. Rep. 9, 20195–17.
742 doi:10.1038/s41598-019-56790-4
743
744 Singh, R., Artaza, J.N., Taylor, W.E., Bhasin, S., Gonzalez-Cadavid, N.F., 2003.
745 Androgens stimulate myogenic differentiation and inhibit adipogenesis in C3H
746 10T1/2 pluripotent cells through an androgen receptor-mediated pathway.
747 Endocrinology 144, 5081–5088. doi:10.1210/en.2003-0741
748
749 Singh, R., Artaza, J.N., Taylor, W.E., Braga, M., Yuan, X., Gonzalez-Cadavid, N.F.,
750 Bhasin, S., 2005. Testosterone inhibits adipogenic differentiation in 3T3-L1 cells:
751 nuclear translocation of androgen receptor complex with beta-catenin and T-cell
752 factor 4 may bypass canonical Wnt signaling to down-regulate adipogenic
753 transcription factors. Endocrinology 147, 141–154. doi:10.1210/en.2004-1649
754
755 Spalding, K.L., Arner, E., Westermark, P.O., Bernard, S., Buchholz, B.A., Bergmann,
756 O., Blomqvist, L., Hoffstedt, J., Näslund, E., Britton, T., Concha, H., Hassan, M.,
757 Rydén, M., Frisén, J., Arner, P., 2008. Dynamics of fat cell turnover in humans.
758 Nature 453, 783–787. doi:10.1038/nature06902
759
760 Tchkonia, T., Morbeck, D.E., Zglinicki, von, T., van Deursen, J., Lustgarten, J.,
761 Scrable, H., Khosla, S., Jensen, M.D., Kirkland, J.L., 2010. Fat tissue, aging, and
762 cellular senescence. Aging Cell 9, 667–684. doi:10.1111/j.1474-9726.2010.00608.x
763

764 Tchkonia, T., Thomou, T., Zhu, Y., Karagiannides, I., Pothoulakis, C., Jensen, M.D.,
765 Kirkland, J.L., 2013. Mechanisms and Metabolic Implications of Regional Differences
766 among Fat Depots. Cell Metab. 17, 644–656. doi:10.1016/j.cmet.2013.03.008
767
768 Teede, H., Deeks, A., Moran, L., 2010. Polycystic ovary syndrome: a complex
769 condition with psychological, reproductive and metabolic manifestations that impacts
770 on health across the lifespan. BMC Med. 8, 41. doi:10.1186/1741-7015-8-41
771
772 Veiga-Lopez, A., Moeller, J., Patel, D., Ye, W., Pease, A., Kinns, J., Padmanabhan,
773 V., 2013. Developmental Programming: Impact of Prenatal Testosterone Excess on
774 Insulin Sensitivity, Adiposity, and Free Fatty Acid Profile in Postpubertal Female
775 Sheep. Endocrinology 154, 1731–1742. doi:10.1210/en.2012-2145
776
777 Wang, L., Li, S., Zhao, A., Tao, T., Mao, X., Zhang, P., Liu, W., 2012. The
778 expression of sex steroid synthesis and inactivation enzymes in subcutaneous
779 adipose tissue of PCOS patients. J. Steroid Biochem. Mol. Biol. 132, 120–126.
780 doi:10.1016/j.jsbmb.2012.02.003
781
782 Weisberg, S.P., McCann, D., Desai, M., Rosenbaum, M., Leibel, R.L., Ferrante,
783 A.W., Jr., 2003. Obesity is associated with macrophage accumulation in adipose
784 tissue. J. Clin. Invest. 112, 1796–1808. doi:10.1172/JCI200319246
785
786 Wensvoort, P., 1967. The development of adipose tissue in sheep foetuses.
787 Path.Vet. 4, 69–78. doi.org/10.1177/030098586700400107
788

Xu, A., Chan, K.W., Hoo, R.L.C., Wang, Y., Tan, K.C.B., Zhang, J., Chen, B., Lam, M.C., Tse, C., Cooper, G.J.S., Lam, K.S.L., 2005. Testosterone selectively reduces the high molecular weight form of adiponectin by inhibiting its secretion from adipocytes. J. Biol. Chem. 280, 18073–18080. doi:10.1074/jbc.M414231200

Yang, X., Jansson, P.-A., Nagaev, I., Jack, M.M., Carvalho, E., Sunnerhagen, K.S., Cam, M.C., Cushman, S.W., Smith, U., 2004. Evidence of impaired adipogenesis in insulin resistance. Biochem. Biophys. Res. Commun. 317, 1045–1051. doi:10.1016/j.bbrc.2004.03.152

Yildirim, B., Sabir, N., Sabir, Kaleli, B., 2003. Relation of intra-abdominal fat distribution to metabolic disorders in nonobese patients with polycystic ovary syndrome. Fertil. Steril. 79, 1358–1364. doi:10.1016/S0015-0282(03)00265-6

Zerradi, M., Dereumetz, J., Boulet, M.-M., Tchernof, A., 2014. Androgens, body fat Distribution and Adipogenesis. Curr. Obes. Rep. 3, 396–403. doi:10.1007/s13679-014-0119-6

Figure legends

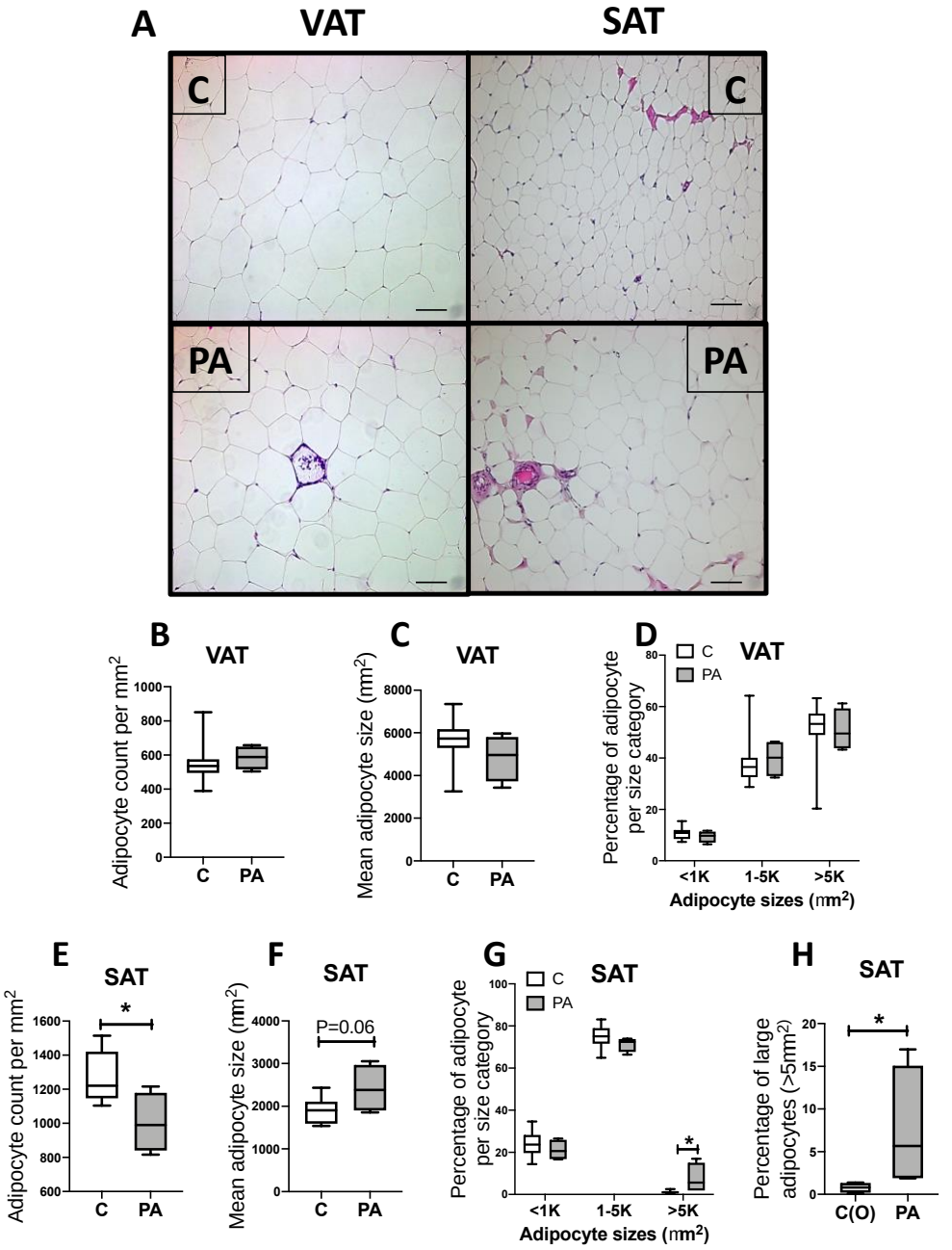

I

	Transcriptional regulators of adipogenesis					
	Visceral adipose tissue			Subcutaneous adipose tissue		
Gene	**C**	**PA**	**P**	**C**	**PA**	**P**
PPARG	0.88 ± 0.25	1.09 ± 0.53	n.s.	1.07 ± 0.41	0.87 ± 0.32	n.s.
CEBPA	1.06 ± 0.43	1.18 ± 0.53	n.s.	1.05 ± 0.38	1.22 ± 0.38	n.s.
CEBPB	1.09 ± 0.47	1.25 ± 0.55	n.s.	1.04 ± 0.30	1.07 ± 0.03	n.s.
CEBPD	1.05 ± 0.36	1.09 ± 0.36	n.s.	1.08 ± 0.44	1.01 ± 0.11	n.s.

Figure 1. Adipose tissue analysis in adult (30M) controls (C; n=11) and prenatally androgenised sheep (PA; n=4). (**A**) Histological analysis of adipocyte morphology in VAT and SAT (C=8; PA=4) (scale bars = 100μm). (**B**) In VAT there was no difference in the numbers of adipocytes per mm^2, (**C**) no difference in the mean size of adipocytes and (**D**) no alteration the number of adipocytes of different sizes. (**E**) PA sheep had decreased number of adipocytes in SAT, (**F**) with a trend to an augmented mean size of adipocytes and (**G**) increased number of large adipocytes. (**H**) The increased number of large SAT adipocytes in PA sheep was still seem when compared to a subset of obese controls (n=4). (**I**) There was no difference in the expression of *PPARG*, *CEBPA*, *CEBPB* and *CEBPD* in adult VAT or SAT. Box plot whiskers are lowest and highest observed values, box is the upper and lower quartile, with median represented by line in box. Data in the table represent mean ± standard deviation. Unpaired, two-tailed Student's t test was used for comparing means of two treatment groups with equal variances accepting $P<0.05$ as significant. (*P<0.05).

A

	Markers of mature adipocytes		
	Visceral adipose tissue		
Gene	**C**	**PA**	**P**
LEP	1.07 ± 0.39	1.22 ± 0.57	n.s.
ADIPOQ	1.09 ± 0.52	1.56 ± 0.97	n.s.
Gene	**Subcutaneous adipose tissue**		
LEP	1.07 ± 0.43	1.29 ± 0.50	n.s.
ADIPOQ	1.08 ± 0.46	1.00 ± 0.25	n.s.

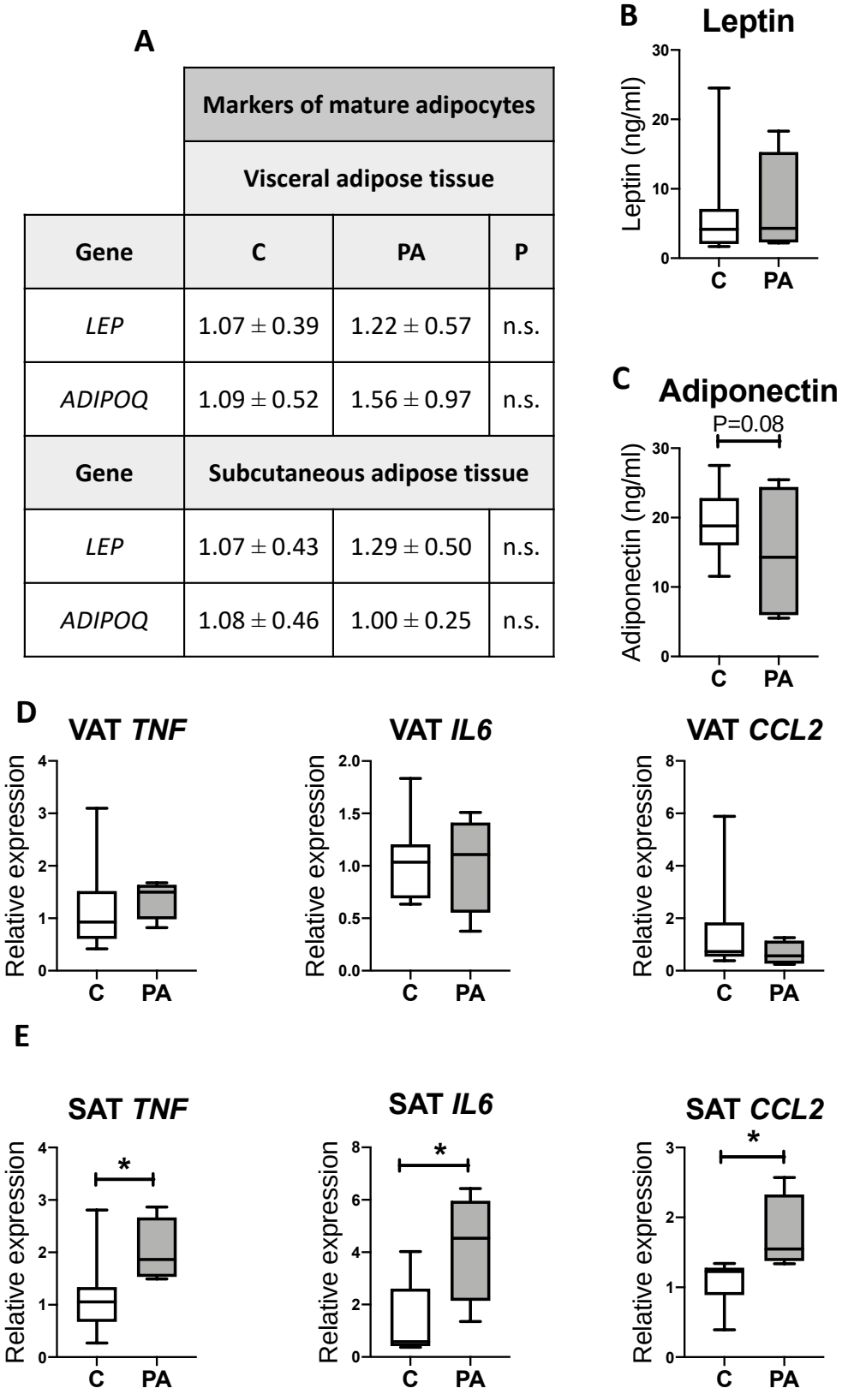

825

826 **Figure 2.** Adipose tissue function in adult (30M) controls (C; n=11) and prenatally
827 androgenised sheep (PA; n=4). (**A**) There were no differences in *LEP* and *ADIPOQ*
828 expression in VAT or SAT. (**B**) There was no difference in the circulating leptin
829 between controls and PA sheep. (**C**) There was a trend towards decreased
830 adiponectin level in PA sheep. (**D**) There were no differences in transcript
831 abundance of inflammatory markers in VAT. (**E**) In SAT PA sheep had increased
832 *TNF*, *IL6* and *CCL2* when compared to controls. Box plot whiskers are lowest and
833 highest observed values, box is the upper and lower quartile, with median
834 represented by line in box. Data in the table represent mean ± standard deviation.
835 Unpaired, two-tailed Student's t test was used for comparing means of two treatment
836 groups with equal variances accepting $P<0.05$ as significant. (*P<0.05).
837

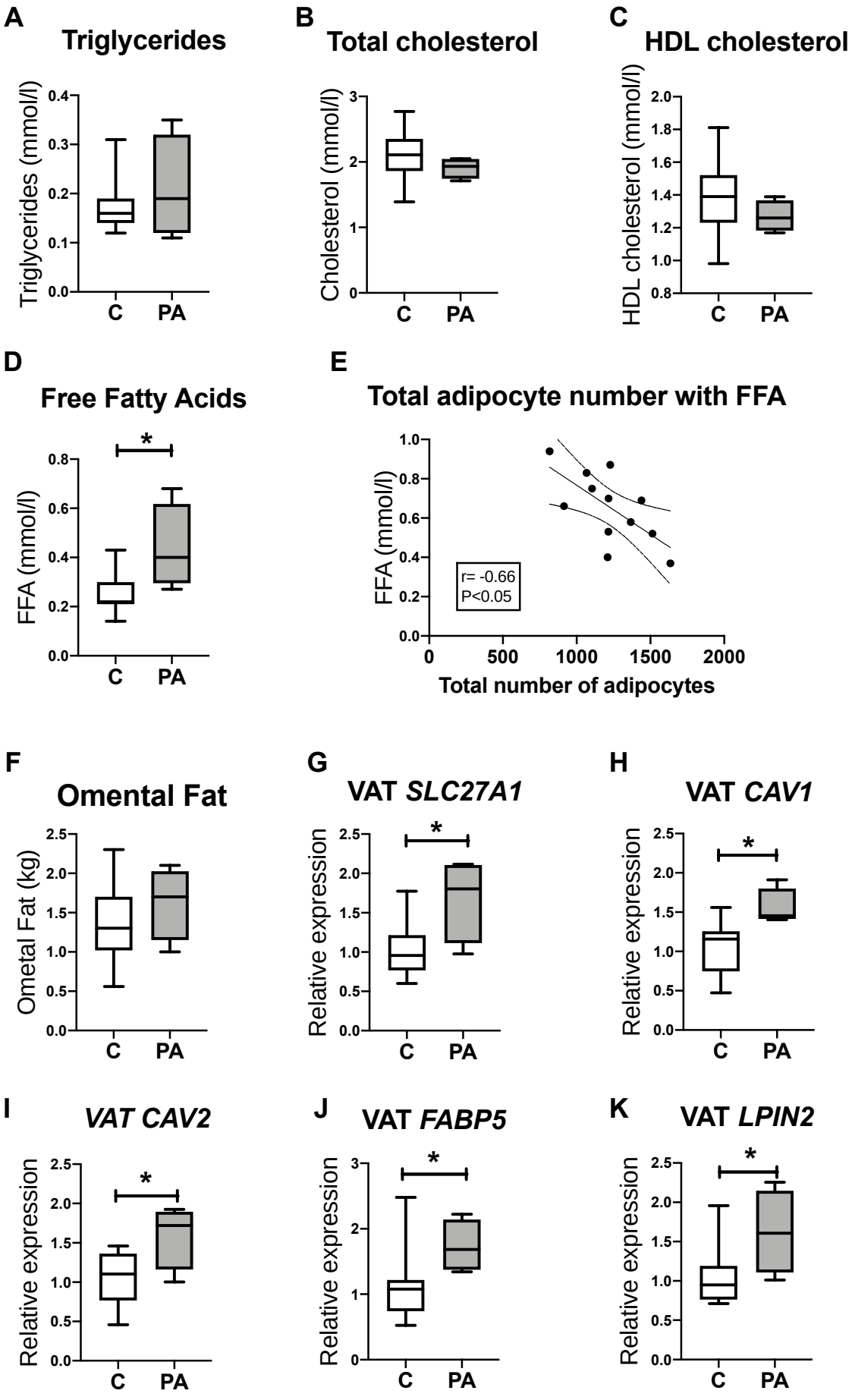
A
Triglycerides
Triglycerides (mmol/l)
0.0
0.1
0.2
0.3
0.4
C
PA
B
Total cholesterol
Cholesterol (mmol/l)
0
1
2
3
C
PA
C
HDL cholesterol
HDL cholesterol (mmol/l)
0.8
1.0
1.2
1.4
1.6
1.8
2.0
C
PA
D
Free Fatty Acids
*
FFA (mmol/l)
0.0
0.2
0.4
0.6
0.8
C
PA
E
Total adipocyte number with FFA
FFA (mmol/l)
r= -0.66
P<0.05
0
500
1000
1500
2000
Total number of adipocytes
F
Omental Fat
Ometal Fat (kg)
0.0
0.5
1.0
1.5
2.0
2.5
C
PA
G
VAT SLC27A1
*
Relative expression
0.0
0.5
1.0
1.5
2.0
2.5
C
PA
H
VAT CAV1
*
Relative expression
0.0
0.5
1.0
1.5
2.0
2.5
C
PA
I
VAT CAV2
*
Relative expression
0.0
0.5
1.0
1.5
2.0
2.5
C
PA
J
VAT FABP5
*
Relative expression
0
1
2
3
C
PA
K
VAT LPIN2
*
Relative expression
0.0
0.5
1.0
1.5
2.0
2.5
C
PA

838

839 **Figure 3.** Metabolic function in adult (30M) controls (C; n=11) and prenatally
840 androgenised sheep (PA; n=4). PCOS-like sheep have normal levels of (**A**)
841 triglycerides, (**B**) cholesterol and (**C**) HDL cholesterol and (**D**) increased circulating
842 FFAs. (**E**) There was negative correlation between the total number of adipocytes
843 per mm^2 and the levels of circulating FFAs. (**F**) At this time there was no difference in
844 omental fat between controls and PA sheep, however there was increased transcript
845 abundance of genes involved in fat uptake and accumulation in VAT (**G**) *SLC27A1*,
846 (**H**) *CAV1*, (**I**) *CAV2*, (**J**) *FABP5* and (**K**) *LPIN2*. Box plot whiskers are lowest and
847 highest observed values, box is the upper and lower quartile, with median
848 represented by line in box. Unpaired, two-tailed Student's t test was used for
849 comparing means of two treatment groups with equal variances accepting $P<0.05$ as
850 significant. Correlation was assessed by calculation of Pearson product-moment co-
851 efficient. (*P<0.05).
852

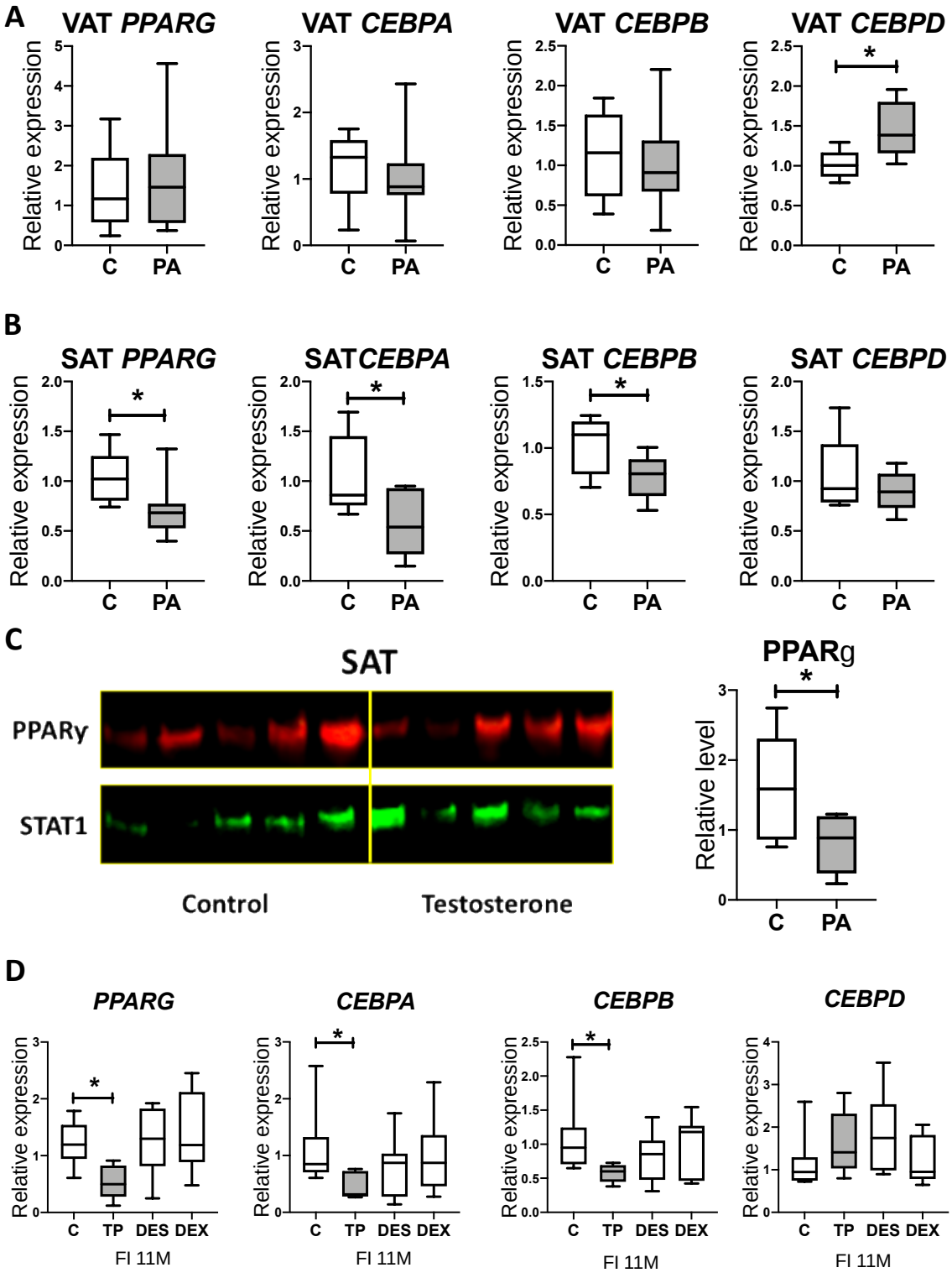

Figure 4. Transcript abundance of adipogenesis markers in adolescent (11M) controls (C; n=5) and prenatally androgenised sheep (PA; n=9). (**A**) In VAT there was no difference in the transcript abundance of *PPARG*, *CEBPA and CEBPB,*

857 although *CEBPD* was increased. (**B**) Prenatally androgenised sheep had decreased
858 adipogenesis in SAT with a reduction in the transcript abundance of *PPARG*,
859 *CEBPA, CEBPB* and no difference in *CEBPD*. (**C**) Decreased level of PPARG in
860 SAT in prenatally androgenised females was confirmed with western blot. (**D**). As
861 compared with controls (C; n=12), the transcript abundance of adipogenesis markers
862 in SAT was decreased by directly injected androgens in fetal life (TP; n=7) but not
863 estrogens (DES; n=8) or glucocorticoids (DEX; n=11). Box plot whiskers are lowest
864 and highest observed values, box is the upper and lower quartile, with median
865 represented by line in box. Unpaired, two-tailed Student's t test was used for
866 comparing means of two treatment groups with equal variances accepting $P<0.05$ as
867 significant. Unpaired, one-tailed Student's t test was used for western blot analysis.
868 For more than two comparisons ANOVA was used with Dunnett's post hoc test.
869 (*P<0.05; ** P<0.01).
870

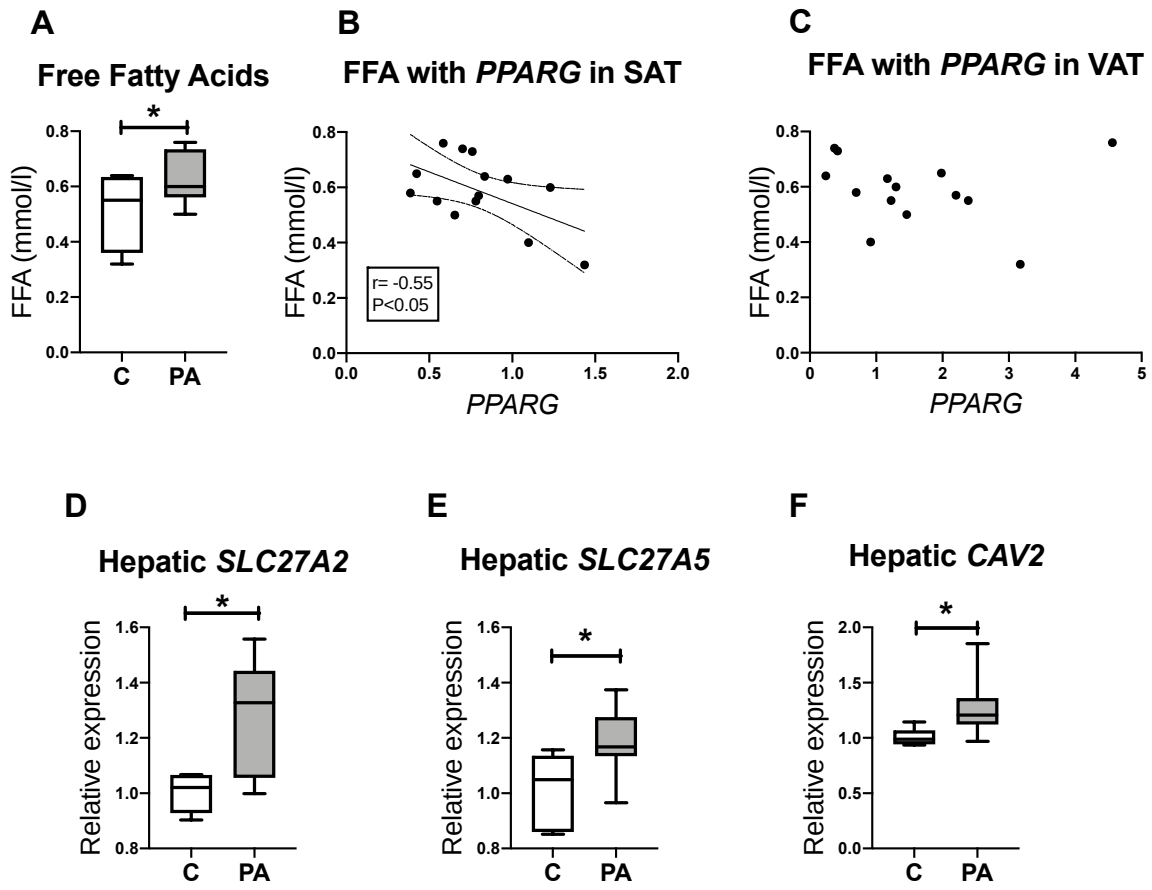

871

872 **Figure 5.** Adipose tissue function in adolescent (11M) controls (C; n=5) and
873 prenatally androgenised sheep (PA; n=9). (**A**) Adolescent prenatally androgenised
874 sheep had increased fasting FFA. (**B**) Concentration of FFAs negatively correlated
875 with *PPARG* (r=-0.55) in SAT but not (**C**) with *PPARG* in VAT. There is increased
876 transcript abundance of (**D**) *SLC27A2*, (**E**) *SLC27A5* and (**F**) *CAV2* involved in
877 hepatic fat uptake. Box plot whiskers are lowest and highest observed values, box is
878 the upper and lower quartile, with median represented by line in box. Unpaired, two-
879 tailed Student's t test was used for comparing means of two treatment groups with
880 equal variances accepting $P<0.05$ as significant. Correlation was assessed by
881 calculation of Pearson product-moment co-efficient. (*P<0.05).

882

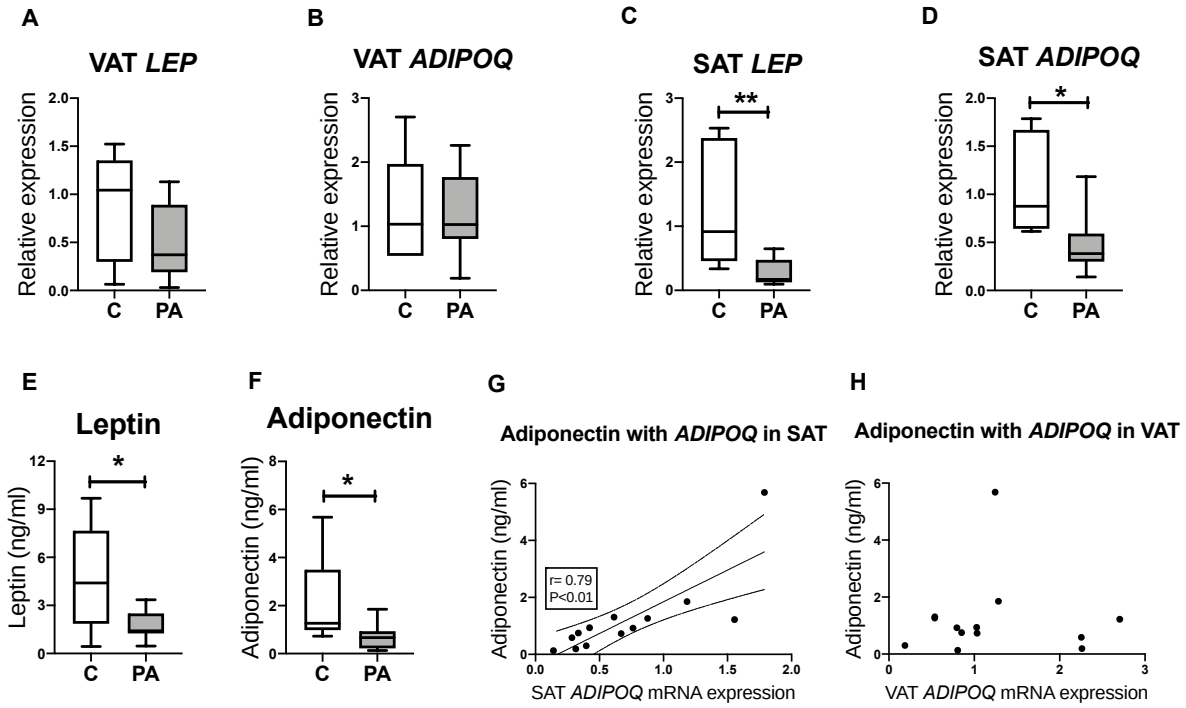

Figure 6. Transcript abundance and circulating levels of leptin and adiponectin in adolescent (11M) controls (C; n=5) and prenatally androgenised sheep (PA; n=9). In VAT there was no difference in the expression of (**A**) *LEP* or (**B**) *ADIPOQ*. Adolescent prenatally androgenised sheep had decreased expression of (**C**) *LEP* and (**D**) *ADIPOQ* in SAT. This was mirrored by a reduction in circulating (**E**) leptin and (**F**) adiponectin in PA sheep. (**G**) Circulating adiponectin correlated (r=0.79) with *ADIPOQ* expression in SAT but not (**H**) in VAT. Box plot whiskers are lowest and highest observed values, box is the upper and lower quartile, with median represented by line in box. Unpaired, two-tailed Student's t test was used for comparing means of two treatment groups with equal variances accepting $P<0.05$ as significant. Correlation was assessed by calculation of Pearson product-moment co-efficient. (*P<0.05; ** P<0.01).

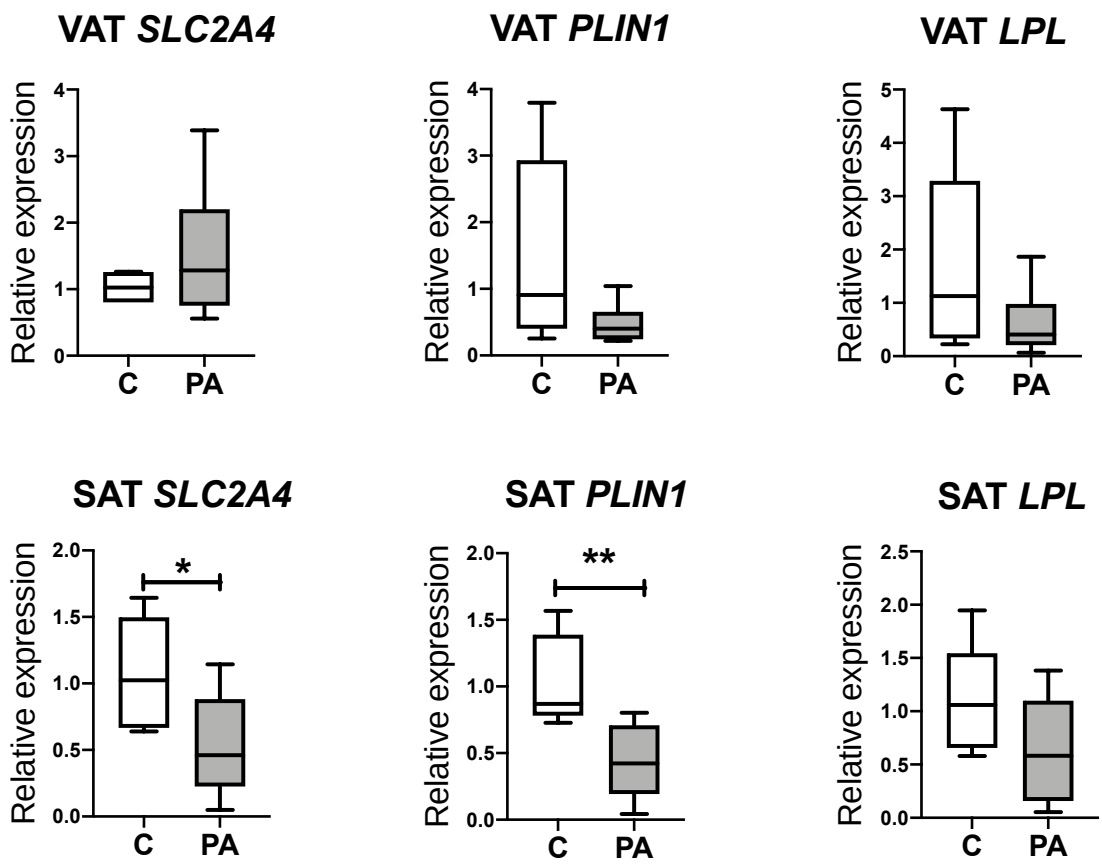

Supplementary Figure 1. Transcript abundance of markers of mature adipocytes in adolescent (11M) controls (C; n=5) and prenatally androgenised sheep (PA; n=9). (**A**) In VAT there was no difference in the transcript abundance of *SLC2A4*, *PLIN1 and LPL*. (**B**) Prenatally androgenised sheep had decreased expression of *SLC2A4* and *PLIN1* in SAT with no difference in *LPL*. Box plot whiskers are lowest and highest observed values, box is the upper and lower quartile, with median represented by line in box. Unpaired, two-tailed Student's t test was used for comparing means of two treatment groups with equal variances accepting $P<0.05$ as significant. (*P<0.05; ** P<0.01).

908 **Table 1**
909

Transcriptional regulators of adipogenesis			
Subcutaneous adipose tissue			
Fetal life (D112)			
Gene	**C**	**TP**	**P**
PPARG	1.29 ± 0.85	1.75 ± 0.39	n.s.
CEBPA	1.26 ± 0.79	1.42 ± 0.63	n.s.
CEBPB	1.21 ± 0.72	1.17 ± 0.55	n.s.
CEBPD	1.05 ± 0.35	1.09 ± 0.19	n.s.
Gene	**Pre-pubertal (11 weeks)**		
PPARG	1.03 ± 0.25	1.30 ± 0.46	n.s.
CEBPA	1.11 ± 0.51	1.47 ± 0.63	n.s.
CEBPB	1.01 ± 0.33	1.34 ± 0.38	n.s.
CEBPD	1.04 ± 0.28	0.90 ± 0.33	n.s.

910

911 **Table 1.** Timing of altered adipogenesis**.** There was no difference in the expression
912 of transcription factors involved in adipogenesis in fetal life at GD112 (C; n=9; PA;
913 n=4) or in pre-pubertal sheep at 11 weeks of age (C; n=8; PA; n=8). Data in the table
914 represent mean ± standard deviation. Unpaired, two-tailed Student's t test was used
915 for comparing means of two treatment groups with equal variances accepting $P<0.05$
916 as significant.

917

Supplementary Table 1

Gene	Forward Primer	Reverse Primer
18S	CAACTTTCGATGGTAGTCG	CCTTCCTTGGATGTGGTA
ACTB	ATCGAGGACAGGATGCAGAA	CCAATCCACACGGAGTACTTG
ADIPOQ	AGAGATGGCACCCCTGGT	GACCTTCGATCCCAGTGATT
ADIPOR1	TCTCCTGGCTCTTCCACACT	AGCTCCCCATGATCAGCA
ADIPOR2	AGGTCGGGAGCCTCTTGTAG	TGAACCCCTCATCTTCCTGA
CAV1	CATCTCTACACTGTTCCCATCC	ACGTCGTCGTTGAGATGCTT
CAV2	CCACAGCAGCGTCGATTAC	CACTGGCTCTGCAATCACAT
CCL2	GACCCCAACCTGAAATGGGT	GCAGTTAGGGGAAGCCAGAA
CEBPA	GTGGACAAGAACAGCAACGA	CGCAGTGTGTCCAGTTCG
CEBPB	GACAAGCACAGCGACGAGTA	AGCTGCTCCACCTTCTTCTG
CEBPD	CGAGTACCGGCAGCGAC	GTCGCGCAGTCCGGC
FABP5	TTCAGCAGCTGGTAGGAAGA	GCACCTACTTTTCGCAGAGC
IL6	AAATGACACCACCCCAAGCA	CTCCAGAAGACCAGCAGTGG
INSR	CACCATCACTCAGGGGAAAC	CAGGAGGTCTCGGAAGTCAG
IRS1	ATCATCAACCCCATCAGACG	GAGTTTGCCACTACCGCTCT
IRS2	TCCAGAACGGCCTCAACTAC	TCAGGTGATGCGTCAAGAAG
LEP	ATCTCACACACGCAGTCCGT	CCAGCAGGTGGAGAAGGTC
LPIN2	GACGTCACCCTGTCACTCTG	GAGTCCAGGGTTTTCTGCAA
MDH1	TTATCTCCGATGGCAACTCC	GGGAGACCTTCAACAACTTTCC
PPARG	TGCAGTGGGGATGTCTCATA	CAGCGGGAAGGACTTTATGT
RPS26	CAAGGTAGTCAGGAATCGCTCT	TTACATGGGCTTTGGTGGAG
SLC27A2	GTGGAAAGGGGAAAATGTGG	TCAAATTCATGGTCTGCCTTC
SLC27A5	CGGACATCAAGTTGCGAAG	ATCCCTGATACCTGCAGCAC
SLC2A4	CCAGCATCTTTGAGTCAGCA	CAGAAGCAGAGCCACAGTCA
TNF	GGTGCCTCAGCCTCTTCT	GAACCAGAGGCCTGTTGAAG

Supplementary Table 1. Primers for real-time RT-PCR analysis. Forward and reverse primers were designed using Primer3 Input version 0.4 online software (http://frodo.wi.mit.edu) with DNA sequences obtained at Ensembl Genome Browser. To confirm the validity of the gene product in the sheep, both conventional PCR and amplicon sequencing were performed. Primer specificity and efficacy for qRT-PCR was evaluated through the generation of standard curves with serial dilutions of

926 cDNA; a standard curve slope of approximately -3.3 was accepted as efficient, and a
927 melt-curve analysis was also performed.